Evaluation of two-group interfacial area transport equation model for vertical small diameter pipes against high-resolution experimental data

Dave, A.; Manera, A.; Beyer, M.; Lucas, D.; Bernard, M.;

Originally published:

January 2017

Chemical Engineering Science 162(2017), 175-191

DOI: https://doi.org/10.1016/j.ces.2017.01.001

Perma-Link to Publication Repository of HZDR:

https://www.hzdr.de/publications/Publ-24231

Evaluation of two-group interfacial area transport equation model for vertical small diameter pipes against high-resolution experimental data.

Akshay J. Dave[a,*], Annalisa Manera[a], Matthias Beyer[b], Dirk Lucas[b], Matthew Bernard[c]

[a] *Department of Nuclear Engineering and Radiological Sciences, University of Michigan, Ann Arbor, MI 48105, USA*
[b] *Helmholtz-Zentrum Dresden-Rossendorf, Institute of Fluid Dynamics, 01314 Dresden, Germany*
[c] *U.S. Nuclear Regulatory Commission, Washington, DC 20555, USA*

Abstract

Two-phase flow is ubiquitous in industrial, chemical and thermal plants alike. The current state-of-the-art system-code model for predicting fluid transport in two-phase flows is the two-fluid model. In the two-fluid transport model, the coupling of mass, momentum and energy transfer between phases is highly dependent on interfacial area transfer terms. Several research efforts in the past have been focused on the development of an interfacial area transport equation model (IATE) in order to eliminate the drawbacks of static regime flow maps currently used in best-estimate thermal-hydraulic system codes. The IATE attempts to model the dynamic evolution of the vapor/liquid interface by accounting for the different interaction mechanisms affecting gaseous phase transport.

The further development and validation of IATE models has been hindered by the lack of adequate experimental data in regions beyond the bubbly flow regime. At the Helmoltz-Zentrum Dresden-Rossendorf (HZDR) experiments utilizing wire-mesh sensors have been performed over all flow regimes, establishing a database of high-resolution (in space and time) data. A 52.3 mm diameter pipe with a 16 by 16 wire-mesh sensor operating at 2.5 kHz is utilized in the air-water experimental database used in this work. There are a total of 37 tests (with varying superficial gas and liquid velocities, at approximately 0.25 MPa). Analysis of IATE performance in the bubbly flow and slug flow regimes is presented.

The performance of the Fu-Ishii two-group IATE model is evaluated. In all regions, the interfacial area concentration for small bubbles is predicted well. The model performs poorly in high void fraction regimes, in which large irregularly shaped bubbles are present. The interaction mechanisms that support and deter performance of the IATE model are highlighted. A sensitivity analysis indicates modification of the group-2 wake entrainment coefficient may extend the validity of the Fu-Ishii model. An optimization study is presented to further explore improving IATE performance. It is concluded that the availability of accurate data at high void fractions from the HZDR facility provides a path to improve IATE performance.

Keywords: Interfacial area transport, Wire-mesh sensor, Small-diameter, Genetic algorithm

1. Introduction

The two-fluid transport model is widely used in best-estimate themal-hydraulic system codes. A complete description of two-phase flow is achieved through the two-fluid model [15], which transports the gas and liquid phase separately. Several formulations of the two-fluid models exist. In the most widely used 6-equation formulation, three equations (mass, momentum and energy) are solved for each phase, resulting in a total of six partial differential equations. Compared to 5-(one momentum equation) or 4-equation (one momentum, one energy equation) formulations, the 6-equation formulation is more accurate for transients in which flow conditions are rapidly changing

*Corresponding Author
Email address: akshayjd@umich.edu (Akshay J. Dave)

Nomenclature

a_i	Interfacial area concentration
α_g	Total void fraction
$\delta(a_i)$	Error in prediction of group-wise or total a_i, Eq. (7)
$\delta(C)$	Relative change in coefficient, Eq. (12)
$\Delta(f(\vec{x}))$	Change in objective function, Eq. (11)
η_{ph}	Volume generation by nucleation
ϕ_j	Interaction mechanism source/sink terms
ϕ_{ph}	Boiling source term
$\vec{v}_g$	Gas velocity
$\vec{v}_i$	Interfacial velocity
D_c	Critical diameter
D_{sm}	Sauter mean diameter
$f(\vec{x})$	Objective function, Eq. (9)

and non-equilibrium field values exist for the phases. For example, the time lag of energy transfer at the interface may cause temperature differences between the gas and liquid phase, which can only be taken into account if two separate energy equations are solved.

The importance of accurate multiphase modelling is not limited to the nuclear plant. Conventional power plants and pharmaceutical plants also experience multiphase transport in their working fluid. For chemical processes and efficient heat transfer properties, the low void fraction regime has been attractive [40]. In chemical reactions, a high interfacial area concentration provides greater yields; for heat transfer, nucleate boiling allows high heat transfer rates. High void fraction flows are also found in several industrial applications. Separation of gas and oil in the petrochemical industry occurs in the churn-turbulent flow regime.

In the two-fluid model, several closure relationships are needed for the interfacial transfer terms which couple the gas and liquid equations. As described by Ishii and Kim [14], closure relationships can be generalized by,

$$(\text{Interfacial Transfer Term}) \propto a_i \cdot (\text{Driving Force}) \ , \tag{1}$$

in which the interfacial area concentration, a_i, represents the surface area per unit volume between the gas and liquid phase. As interfacial transfer terms for mass, momentum, and energy couple the two phases in the two-fluid model, the importance of correctly predicting interfacial area concentration is evident.

The interfacial area transport equation (IATE) was initially proposed by Kocamustafaogullari and Ishii in 1995 [23]. Following the initial proposal, a one-group formulation was proposed by Wu in 1998 [51]. In 2001 a two-group model was proposed by Hibiki and Ishii [11], followed in 2003 by a more advanced two-group model by Fu and Ishii [8]. The IATE model attempts to address the shortcomings of the current state-of-the-art method based on static regime flow maps (e.g. [19]). Regime maps rely on algebraic relations for flow-regime transition criteria that are only valid for steady-state fully-developed flow [13]. Dynamic evolution of interfacial structure is not properly captured (e.g. entrance effects and the downstream flow development, transitioning between flow regimes, transient flows). Furthermore, regime maps required both transition criteria and closure relationships, which depend on flow configurations and on the particular geometrical configuration. This led to the additional possibility of compounding error from two sources.

1.1. Interfacial Area Transport Equation Model

Two main formulations of the IATE model have been proposed: a one-group (1G IATE) and a two-group (2G IATE). The development of both formulations was published in 2003 by Ishii and Kim [14]. The 1G IATE is given by

$$\frac{\partial a_i}{\partial t} + \nabla \cdot (a_i \vec{v}_i) = \frac{2}{3}\left(\frac{a_i}{\alpha_g}\right)\left(\frac{\partial \alpha_g}{\partial t} + \nabla \cdot (\alpha_g \vec{v}_g) - \eta_{ph}\right) + \sum_j \phi_j + \phi_{ph} \ . \tag{2}$$

The left hand side of Eq. (2) accounts for the time rate of change and convection of interfacial area concentration. The first right hand side term accounts for the volume expansion of bubbles due to pressure changes, the second term accounts for source/sink terms due to bubble interaction mechanisms and the last term accounts for phase change due to evaporation or condensation.

The 1G IATE bins all bubbles into a single group which presents several disadvantages. For flows containing a large spectrum of bubble sizes, there are varying drag coefficients and differing incidences of bubble interaction mechanisms. Therefore, the one-group model has limited applicability as all bubbles are considered to be spherical in shape, which restricts the validity of the model to the bubbly flow regime only. The 2G IATE accounts for these differences by separating small spherical/distorted bubbles and large irregularly shaped bubbles into two separate groups. Group-1 is represented by

$$\begin{aligned}\frac{\partial a_{i1}}{\partial t} + \nabla \cdot (a_{i1} \vec{v}_{i1}) =& \frac{2}{3}\left(\frac{a_{i1}}{\alpha_1}\right)\left(\frac{\partial \alpha_1}{\partial t} + \nabla \cdot (\alpha_1 \vec{v}_{g1}) - \eta_{ph}\right) - \\ & -C\left(\frac{D_c}{D_{sm1}}\right)^3 \left(\frac{a_{i1}}{\alpha_1}\right)\left(\frac{\partial \alpha_1}{\partial t} + \nabla \cdot (\alpha_1 \vec{v}_{g1}) - \eta_{ph}\right) + \sum_j \phi_{j1} + \phi_{ph1} \ ,\end{aligned} \tag{3}$$

and group-2 is represented by

$$\begin{aligned}\frac{\partial a_{i2}}{\partial t} + \nabla \cdot (a_{i2} \vec{v}_{i2}) =& \frac{2}{3}\left(\frac{a_{i2}}{\alpha_2}\right)\left(\frac{\partial \alpha_2}{\partial t} + \nabla \cdot (\alpha_2 \vec{v}_{g2})\right) + \\ & +C\left(\frac{D_c}{D_{sm1}}\right)^3 \left(\frac{a_{i1}}{\alpha_1}\right)\left(\frac{\partial \alpha_1}{\partial t} + \nabla \cdot (\alpha_1 \vec{v}_{g1}) - \eta_{ph}\right) + \sum_j \phi_{j2} \ .\end{aligned} \tag{4}$$

Eqs. (3) and (4) represent the two-group interfacial area transport equation model. Group-1 consists of small bubbles, assumed to be spherical in shape. Group-2 consists of larger, irregularly shaped bubbles. The border between the two groups is determined by the critical diameter, $D_c = 4\sqrt{\sigma/(g\Delta\rho)}$ [16]. The value of D_c for air-water flows at TOPFLOW conditions (see Section 2) is $\approx$11 mm. There are similarities between the 1G and 2G IATE equations. For 2G IATE, a new term appears on the right hand side with the coefficient C, that accounts for the inter-group transfer between group-1 and group-2 interfacial area. The coefficient C is a distribution parameter which has been shown experimentally to equal unity. A majority of the discrepancies of the formulations are encapsulated in the interaction mechanisms (ϕ_j for 1G IATE and ϕ_{j1}, ϕ_{j2} for 2G IATE). The present study focuses on IATE performance over a wide range of flow regimes. Therefore, emphasis is placed on the validation of the 2G IATE model.

Several models based on the two-group formulation have been proposed in the literature. They differ with regards to their range of applicability and in the degree of complexity. As is the case for many thermal-hydraulic phenomena, a more complex model does not necessarily guarantee better predictive capabilities. IATE models specific to two-phase flows in vertical pipes are summarized in Table 1. Earlier models tend to be simpler in terms of interaction mechanisms covered, such as the Hibiki-Ishii model. The Fu-Ishii model is considered the state-of-the-art model for two-phase flows in small diameter vertical pipes.

In addition to the IATE formulations listed in Table 1, other models can be found in the literature for flows

Table 1: Existing two-group IATE models that are applicable to vertical two-phase flows.

Model	Applicability	Mechanism Exclusion	Parameters
Hibiki-Ishii [11]	Vertical small diameter Bubbly to slug flow	Shearing-off, surface instability, intergroup expansion	12
Fu-Ishii [7, 8]	Vertical small diameter Bubbly to churn-turbulent	Intergroup expansion	11
Smith-Schlegel [44, 41]	Vertical large diameter Bubbly to annular	Intergroup expansion	17
Sun [46]	Vertical rectangular channel Bubbly to annular	None	15

involving phase change, including boiling. Kocamustafaogullari and Ishii [22] included the modelling of active nucleation site density of the heated surface. Hibiki and Ishii [12] modelled nucleation site density using size and angle distribution of cavities present on the heated surface. Bubble departure size was modeled by Situ [43], and bubble departure frequency by Euh [6]. Furthermore, the sink term due to condensation has been modelled by Park [34]. The present study focuses on adiabatic air-water flows and thus does not employ any of these models.

In this study, the two-group Fu-Ishii [7, 8] model will be assessed. A summary of interaction mechanisms that are accounted for in the Fu-Ishii model are presented in Table 2. It is important to note the coefficients that are listed in the last column. These parameters are determined experimentally and affect the incidence of interaction mechanisms. In the literature, a comprehensive review by Liao and Lucas of all postulated two-phase break-up mechanisms [24] and coalescence mechanisms [25] is also available. A recent review on bubble break-up and coalescence mechanisms relevant for the churn-turbulent flow regime has also been published by Montoya [31].

Table 2: List of various interaction mechanisms accounted for in the Fu-Ishii model. All empirical parameters used by each mechanism are listed in the last column [13].

Symbols	Mechanisms	Interaction	Empirical Coefficients
$\phi_{RC}^{(1)}$	Random collision	(1)+(1)→(1)	$C_{RC} = 0.0041$
$\phi_{RC}^{(11,2)}$	Random collision	(1)+(1)→(2)	$C_{RC} = 0.0041$
$\phi_{WE}^{(1)}$	Wake Entrainment	(1)+(1)→(1)	$C_{WE} = 0.002$
$\phi_{WE}^{(11,2)}$	Wake Entrainment	(1)+(1)→(2)	$C_{WE} = 0.002$
$\phi_{WE}^{(12,2)}$	Wake Entrainment	(1)+(2)→(2)	$C_{WE}^{12,2} = 0.015$
$\phi_{WE}^{(2)}$	Wake Entrainment	(2)+(2)→(2)	$C_{WE}^{(2)} = 10.0$
$\phi_{TI}^{(1)}$	Turbulent Impact	(1)→(1)+(1)	$C_{TI} = 0.0085$
$\phi_{TI}^{(2)}$	Turbulent Impact	(2)→(2)+(2)	$C_{TI} = 0.0085$
$\phi_{SO}^{(2,12)}$	Shearing-off	(2)→(1)+(2)	$C_{SO} = 0.031$

In the Fu-Ishii 2G IATE formulation, two coalescence and two break-up mechanisms are taken into account. A graphical depiction of these mechanisms is presented in Fig. 1. The coalescence mechanisms are random collision and wake entrainment. The random collision mechanism accounts for the coalescence due to movements of bubbles driven by turbulent eddies. The wake entrainment mechanism occurs when a bubble enters the wake region of a leading bubble. The trailing bubble may accelerate and collide with the leading bubble, resulting in coalescence. The break-up mechanisms are turbulent impact, shearing-off and surface instability. Turbulent impact occurs if an eddy impacting a bubble is strong enough to overcome the surface tension of the bubble surface, causing break-up. Shearing-off is a complex mechanism that arises for large bubbles and is one of the least understood mechanisms. It occurs for large bubbles that form a skirt at the base of the bubble. It is postulated that disruptive viscous forces pulling at the rim of the skirt overwhelm the local cohesive surface tension and form small group-1 bubbles. Surface

instability occurs when a bubble grows and reaches a limit at which the leading interface can no longer be sustained because of turbulence-induced instabilites. The surface instability mechanism was found to be insignificant and was therefore absorbed into the turbulent impact mechanism for group-2. A derivation of each mechanism is available in the literature [8] and extensively detailed in [13]. The Fu-Ishii model is specifically developed for adiabatic bubbly, slug and churn-turbulent flow for vertical small-diameter pipes. The inter-group bubble expansion is ignored in the Fu-Ishii model as experiments [20] have shown that the shearing-off mechanism dominates inter-group transfer.

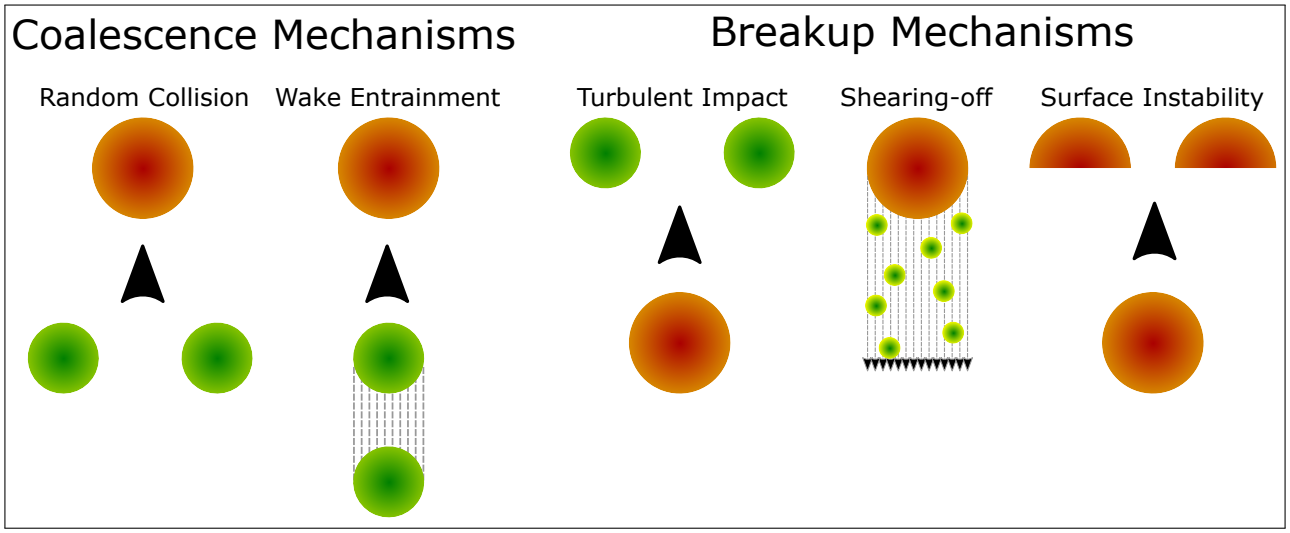

Figure 1: An overview of bubble interaction mechanisms that are considered by the interfacial area transport equation model. Vertical orientation indicates the upstream position of the bubbles during the interaction. Color indicates relative expected bubble size.

The objective of the present study is to evaluate the Fu-Ishii 2G IATE model against a small-diameter high-resolution high-frequency wire-mesh sensor database. A review of past experiments and validation efforts is presented in Section 1.2. The wire-mesh sensor database used in the present study is introduced in Section 2. An evaluation of the Fu-Ishii model against the wire-mesh sensor experimental database is presented in Section 3. Lastly, results from optimization studies using all databases available in the literature is summarized in Section 4. Concluding remarks are noted in Section 5.

1.2. Previous Validation Efforts

The databases that have been published in the literature for vertical-upward small-diameter pipes is presented in Table 3. The majority of databases published by other authors utilize the needle probe sensor as the experimental measurement tool. The needle probe sensor is an intrusive measurement technique and was originally proposed by Neal and Bankoff [32]. These sensors are used to measure the time-averaged local void fraction on the basis of local conductivity (conductivity needle probes) or optical properties of the gas/liquid phases (optical probes). Several designs have been proposed for this type of sensor: a two-sensor probe [50], a four-sensor probe [21], and a five-sensor probe [5]. A double sensor probe allows the measurement of the interface velocity in addition to the local void-fraction. This type of sensor is mostly suitable for bubbly flows. Four- and five-sensor probes can be also applied to more complex high-void fraction conditions. They allow for the measurement of the inclination angle of the liquid-gas interface, which can be used for an indirect measurement of the interfacial area concentration.

The Fu-Ishii two-group model's coefficients were evaluated with air-water experiments for a vertical 48.3 mm diameter pipe [7]. The coefficients for group-1 were consistent with those of the one-group IATE model [51]. New group-2 coefficients were determined. The experimental data on local void-fraction, bubble velocity and interfacial area were measured using four-sensor conductivity probes at 5, 30 and 55 L/D. The experiments covered the bubbly

Table 3: Summary of existing experimental database suitable for vertical-upward small-diameter interfacial area transport equation development. Regimes: (1) bubbly, (2) slug, (3) churn-turbulent, (4) annular. The experimental data that is benchmarked in Section 3 is highlighted.

Database	Sensor Type	Pipe Diameter [mm]	Tests	Measurement L/D	Regimes
Ishii [17]	Double/four-tip needle probe	12.7	9	17, 120, 217	(1)
Fu [7]	Four-tip needle probe	48.3	19	5, 30, 55	(1), (2)
Worosz [49]	Four-tip needle probe	50.8	9	18, 35, 63	(1), (2)
Prasser [38]	Wire-mesh	52.3	37	2, 31, 59, 151	(1), (2)
Ishii [17]	Double/four-tip needle probe	102	19	5, 20, 30	(1), (2)

and slug flow regime. Across the two flow regimes, the average error of the Fu-Ishii 2G IATE model for the prediction of interfacial area concentration was found to be 10%, and 15%, respectively.

In an attempt to improve the predictive capability of the 6-equation two-fluid model, the IATE model has been implemented in a development branch of the best-estimate thermal-hydraulics system code TRACE, developed by the US Nuclear Regulatory Commission. Initially, the 1G IATE model was implemented by Talley [47] in TRACE v4.291b. The experimental dataset contained vertical-downward bubbly flow regime air-water experiments for 25.4 mm and the Fu experiments (vertical-upward 48.3 mm pipe). The study concluded that the 1G IATE improved a_i prediction in TRACE from an average of $\pm 48\%$ to $\pm 8\%$. The 2G IATE model was implemented in TRACE v5.0p3 by Bernard [1]. The performance was validated against air-water experiments the same 48.3 mm Fu database. Since the two-group model is implemented, the study evaluated bubbly and slug flow regime. The study concluded that the 2G IATE improved a_i prediction in TRACE from an average of $\pm 42\%$ to $\pm 19\%$ for all tests. For bubbly flow the average error was $\pm 10\%$, which is similar to the error cited in the 1G IATE TRACE study by Talley. However, Bernard's study noted that a_i prediction in the high void fraction regimes remained challenging. Worosz [49] has proposed a model that changes from 1-group to 2-group IATE when transitioning from the bubbly to slug flow regime. Thus, the experimental data introduced by Worosz only focuses on the transition region (see Fig. 2 for expected flow regimes). Two other experimental databases by Ishii [17] (of 12.7 mm and 102 mm) exist. However, they significantly deviate from the ≈ 50 mm hydraulic diameter for which the coefficients of the Fu-Ishii model were evaluated.

1.3. 2G IATE implementation

The objective of this study is to assess the performance of the Fu-Ishii 2G IATE model against a database of high resolution wire-mesh sensor data (noted as Prasser [38] in Table 3) for air-water flows in a vertical small-diameter pipe over a wide range of void fractions. In this subsection, the numerical implementation of the 2G IATE model is discussed. Several assumptions allow simplification of the two interfacial area transport equations (Eqs. (3) and (4)). The first assumption is that the axial evolution of a_i does not vary with time (steady-state). The second assumption is that no phase-change occurs. Both conditions are valid due to the experimental operating conditions presented in the next section. A third assumption is that the velocity at the gas-liquid interface is equivalent to the bulk velocity of the gas (i.e. $v_i \approx v_g$). The final assumption is that all field variables are approximately constant in the cross-section of the pipe – they only vary in the axial direction. This assumption allows a one-dimensional formulation of the two-group interfacial area transport equation. The simplified equation for group-1 is

$$\frac{\partial}{\partial z} a_{i1} v_{g1} = \frac{2}{3}\left(\frac{a_{i1}}{\alpha_1}\right)\left(\frac{\partial}{\partial z}\alpha_1 v_{g1}\right) - C\left(\frac{D_c}{D_{sm1}}\right)^3\left(\frac{a_{i1}}{\alpha_1}\right)\left(\frac{\partial}{\partial z}\alpha_1 v_{g1}\right) + \sum_j \phi_{j1} \ , \tag{5}$$

and group-2 is represented by

$$\frac{\partial}{\partial z} a_{i2} v_{g2} = \frac{2}{3}\left(\frac{a_{i2}}{\alpha_2}\right)\left(\frac{\partial}{\partial z}\alpha_2 v_{g2}\right) + C\left(\frac{D_c}{D_{sm1}}\right)^3\left(\frac{a_{i1}}{\alpha_1}\right)\left(\frac{\partial}{\partial z}\alpha_1 v_{g1}\right) + \sum_j \phi_{j2} \ . \tag{6}$$

The structure of both group-1 and group-2 equations is similar. The left-hand side accounts for the axial rate of change of group-wise interfacial area concentration, a_i. The first right-hand side term accounts for change in a_i due to group-wise void fraction evolution (attributed to pressure-drop expansion). The second right-hand side term accounts inter-group transfer due to group-1 void fraction evolution. The last right-hand side term accounts for group-wise change in a_i due to bubble interaction mechanisms.

There are a total of six unknown variables in Eqs. (5) and (6) (i.e. group-wise values of α_g, a_i and v_g), and therefore four more equations are necessary for closure. The two-fluid model [15] can be used to close the interfacial area transport equation. However, the two-fluid model only provides an estimate for group-wise α_g and v_g. On the other hand, the wire-mesh sensor data (presented in Section 2) provides *experimental* group-wise α_g, a_i and v_g values at several axial locations (2, 31, 59 and 151 L/D). A quadratic fit (with respect to axial location) to these field values accurately captures their advection. Using the experimental values of α_g and v_g for closure of the 2G IATE will allow a better isolation of error. Thus, the error in predicting a_i can be attributed solely to the formulation of the 2G IATE model (and not hindered by any inaccuracies in the two-fluid model).

In order to solve Eqs. (5) and (6), they were discretized using a first order forward difference scheme. A mesh convergence study determined that mesh size $dz = 0.1\,\mathrm{m}$ was sufficient. The initial condition for the group-wise a_i is taken from the experimental data measured at the first axial location. In the results section (Section 3.2), the performance of 2G IATE will be quantified by the error

$$\delta(x) \equiv \frac{1}{N-1}\sum_{n=2}^{N}\left|\frac{x_{n,calc}-x_{n,meas}}{x_{n,meas}}\right| \,, \tag{7}$$

where $x_{n,calc}$ and $x_{n,meas}$ are the calculated and measured values, respectively, at the n-th axial location. The error in predicting group-wise and total interfacial area will be discussed. Hewitt studied and identified the regimes in vertical two-phase annular flow in 1970 [10]. In 1984, the quantification of regime transitions were proposed by Mishima and Ishii [29]. The regime map (based on experimental operating conditions of data presented in this study) is produced in Fig. 2.

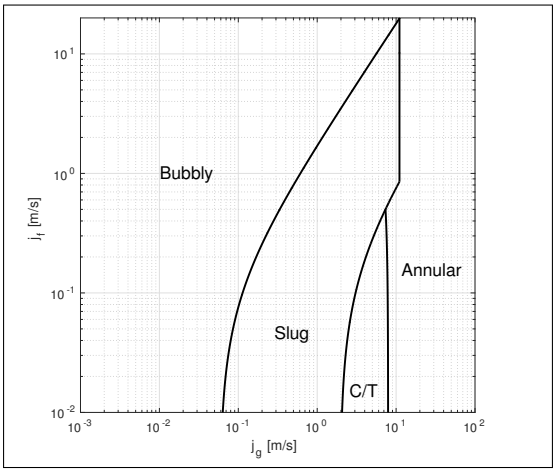

Figure 2: Anticipated flow regimes in DN50 TOPFLOW tests.

2. Experimental Data

The objective of this study is to assess 2G IATE performance against a high resolution experimental database that covers both low and high void fraction two-phase flow regimes. The experimental database is obtained from the TOPFLOW facility at Helmholtz-Zentrum Dresden-Rossendorf [38]. The experimental facility consists of a vertical

8.0 m long, 52.3 mm diameter test section. A visual of the TOPFLOW facility test section is presented in Fig. 3. A sparger with eight 4 mm orifices that is located at the center of the test section inlet was used for gas injection. The water was fed in the test section from the bottom side. Wire-mesh sensors (WMS) are used to measure two-phase flow parameters at four locations along the vertical axis of the test section (at 1.91, 30.6, 59.3, and 151 L/D). Thus, the axial development of air-water flow over 8.0 m can be characterized. The experimental test matrix is reported in Table 4. Test cases that have been conducted at TOPFLOW are highlighted in bold and classified according to the flow regime. All tests are operated at approximately 0.25 MPa. The WMS enables measurement of local void fraction over an array of 16 by 16 locations in the pipe cross-section with a spatial resolution of 3 mm and an acquisition frequency of 2.5 kHz. Details on the working principle of the WMS is provided by Prasser [35].

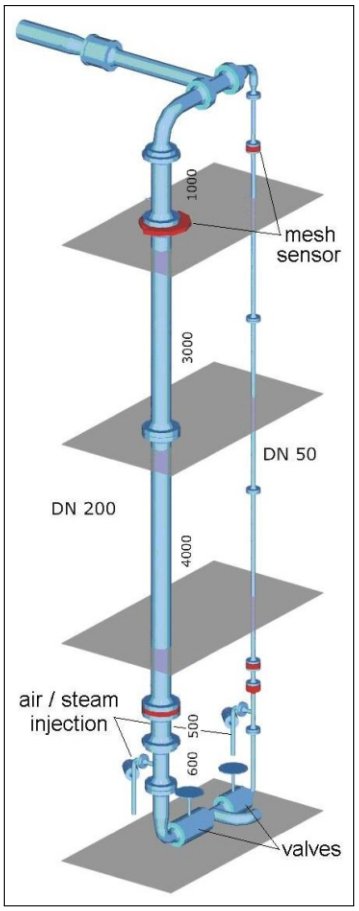

Figure 3: A visual of the DN50 TOPFLOW test section. A full report of the experiments and test facility is available [38].

Several studies have focused on the comparison between WMS and non-intrusive methods such as: high-speed camera [36], ultra-fast X-ray tomography [37, 52], and gamma densitometry [39, 27, 26, 42]. Comparisons with high-speed camera has shown that in case of air-water flows, WMS have a significant effect on the flow structure downstream of the sensor (bubbles are cut by the WMS electrodes), but the WMS signal is representative of the undisturbed flow. The effect on the bubble shape disappears with decreasing surface tensions, as observed in applications involving steam-water flows [27, 26]. The quantitative comparisons between WMS and time-resolved X-ray tomography have shown good agreement for the measurement of both void fraction and gas velocity profiles. Good agreement with the void-fraction obtained with gamma densitometry has also been found. Quantitative studies of the impact of WMS in case of air-water mixtures at atmospheric pressure [48] indicate significant changes to the velocity profile downstream of the sensor particularly at low gas velocities. However, comparisons with

ultra-fast Xray tomography [37] have demonstrated that the velocity and void fraction profiles measured by the WMS is that of the undisturbed flow.

A comparison of WMS measurements to needle probe sensors has also been conducted by Manera [28]. The devices had good agreement (in measurement of a_i) at low void-fraction conditions, but appreciable disagreement was observed at higher void fractions. For smaller bubbles ($D_b \leq 10\,\text{mm}$), there is good agreement between WMS and the needle probe sensor. For higher void fraction, there is a large discrepancy towards the center of the pipe (larger bubbles/slugs aggregate towards the center of the pipe for small diameter pipes), where the measurement of the needle probe exhibits erratic behavior, probably due to the lack of sufficient counts (i.e. poor statistics).

The experimental data that has been used to develop and validate IATE models have been mostly based on measurements with conductivity probes. The WMS provides several benefits over the conductivity probes. Since the data is acquired at a high spatial resolution, the duration of the experiments is significantly reduced (approximately 10 s for a test point versus several hours for the conductivity probe). Bubble velocity is measured using a pair of WMS mounted in successive order. Combining the 2D void fraction and velocity measurements, a full reconstruction of the liquid-gas interface can be achieved (within the limit of the sensor's spatial resolution) allowing 3D visualization of the measured flow. Furthermore, the ability to gather accurate [2] two-phase flow data over a wide range of flow regime is invaluable (high void fraction flow regimes is challenging for conductivity probes due to the parallel alignment of the gas-liquid interface).

Table 4: Experimental test matrix for the DN50 TOPFLOW tests. Test numbers with colored font have been conducted experimentally and are covered in the present study. Font color indicates an experimentally observed flow regime.

Superficial liquid velocity [m/s]	Superficial gas velocity [m/s]															
	0.0025	**0.0040**	**0.0062**	**0.0096**	**0.0151**	**0.0235**	**0.0368**	**0.0574**	**0.0898**	**0.140**	**0.219**	**0.342**	**0.534**	**0.835**	**1.305**	**2.038**
4.047	11	22	33	44	55	66	77	88	99	110	121	132	143	154	165	176
2.554	10	21	32	43	54	65	76	87	98	109	120	131	142	153	164	175
1.611	9	20	31	**42**	53	64	75	86	97	108	**119**	130	141	152	163	174
1.017	**8**	19	**30**	**41**	**52**	**63**	**74**	**85**	**96**	**107**	**118**	**129**	**140**	**151**	**162**	173
0.641	7	18	29	**40**	51	62	73	84	95	106	**117**	128	139	150	161	172
0.405	**6**	17	**28**	**39**	**50**	**61**	**72**	**83**	**94**	**105**	**116**	**127**	**138**	**149**	**160**	171
0.255	5	16	27	**38**	49	60	71	82	93	104	**115**	126	137	148	159	170
0.161	4	15	26	**37**	48	59	70	81	92	103	**114**	125	136	147	158	169
0.102	3	14	25	**36**	47	58	69	80	91	102	113	124	135	146	157	168
0.0641	2	13	24	35	46	57	68	79	90	101	112	123	134	145	156	167
	Bubbly Flow											**Slug Flow**				

3. Evaluation of WMS Database

The Fu-Ishii 2G IATE model (Section 1.3) is evaluated against the TOPFLOW DN50 experimental database (introduced in Section 2). An overview of the IATE performance is presented in Section 3.1, highlighting flow conditions that challenge the model. A detailed discussion of mechanisms that contribute to succesful and poor performance of IATE is given in Section 3.2. A sensitivity analysis of the coefficients of the Fu-Ishii model is presented in Section 3.3.

3.1. Overview

The error in predicting interfacial area concentration, calculated using Eq. (7), is presented for the entire DN50 TOPFLOW database in Fig. 4. In this figure, the error in prediction of group-1, group-2 and total interfacial area

are presented separately. Tests that have no large group-2 bubbles are omitted in presentation of group-2 error. The prediction of group-1 a_i is generally good in the bubbly flow regime and deteriorates towards the slug flow regime. A similar trend is noted for group-2 a_i error, however, the magnitude is significantly higher, with most cases being well above 80%. The error for the prediction of total a_i follows a similar qualitative trend. Due to the poor performance of group-2 a_i in the slug flow regime, the error in total a_i can be larger than $> 30\%$.

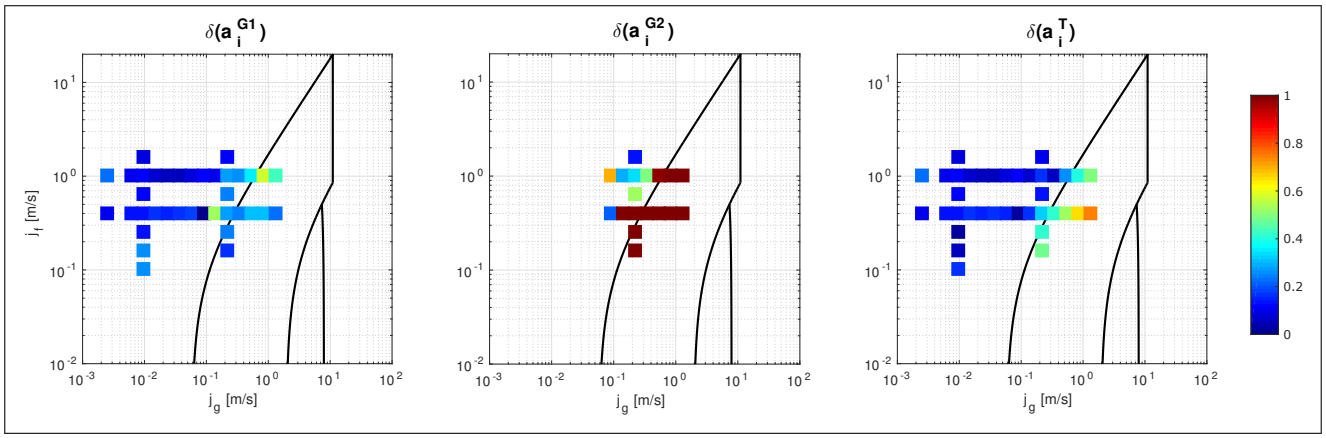

Figure 4: A comparison of performance for DN50 TOPFLOW data. Left column indicates error for group 1 interfacial area concentration and center column indicates error for group 2 interfacial area concentration. The right column indicates error for prediction of total interfacial area.

It can be concluded that, in general, the IATE model struggles in high void fraction regimes. The propagation of group-2 a_i is incorrect in the majority of the tests. For group-1, further investigation is necessary to determine the impact of varying superficial velocities on the incidence of interaction mechanisms. Isolating sources of error may provide insight into how to improve IATE performance.

3.2. Discussion

A comparison of the predicted interfacial area using the Fu-Ishii 2G IATE model against experimental data is presented for selected tests in Figs. 5 to 8. In the figures, the results of the IATE model are indicated with continuous lines and the experimental values are indicated with cross symbols. Group-1 interfacial area and void fractions values are reported in red, group-2 values in blue, and total in black. Cumulative source term contributions (Δa_i^{G1}, and Δa_i^{G2}) from IATE interaction mechanisms (ϕ_{j1}, and ϕ_{j2}) are also presented. To provide further insight, the experimental axial development of bubble size distributions is also reported.

At low superficial gas and liquid velocities, the flow is strictly in the bubbly flow regime. The results for Test 30, corresponding to the bubbly flow regime, is presented in Fig. 5. The qualitative propagation of the interfacial area concentration, a_i, is good. Quantitatively, the a_i predicted downstream is within the $\pm 10\%$ measurement uncertainty. No large group-2 bubbles are present in these conditions. The group-1 bubble interaction mechanism source terms are negligible, as indicated by their absence in Δa_i^{G1}. The dominating source term is the group-1 bubble expansion term (first term on the right hand side of Eq. (3)). In steady state adiabatic air-water flows this term simplifies to

$$\phi_{EXP} = \frac{2}{3}\left(\frac{a_i}{\alpha_g}\right)\frac{\partial}{\partial z}\alpha v_g \ . \tag{8}$$

The bubble expansion term relies on good prediction of void fraction and gas phase velocity. As both these field values are directly interpolated from experimental data, the predicted a_i value is expected to be accurate. This result suggests that for simple volumetric expansion and no bubble interaction mechanisms, the dynamics of two-phase flow is correctly captured. The bubble size distribution does not change significantly along the axis of the

pipe. The width of the distribution contracts at 59 L/D then shifts towards higher diameters at 151 L/D – further supporting the predicted propagation of bubble expansion.

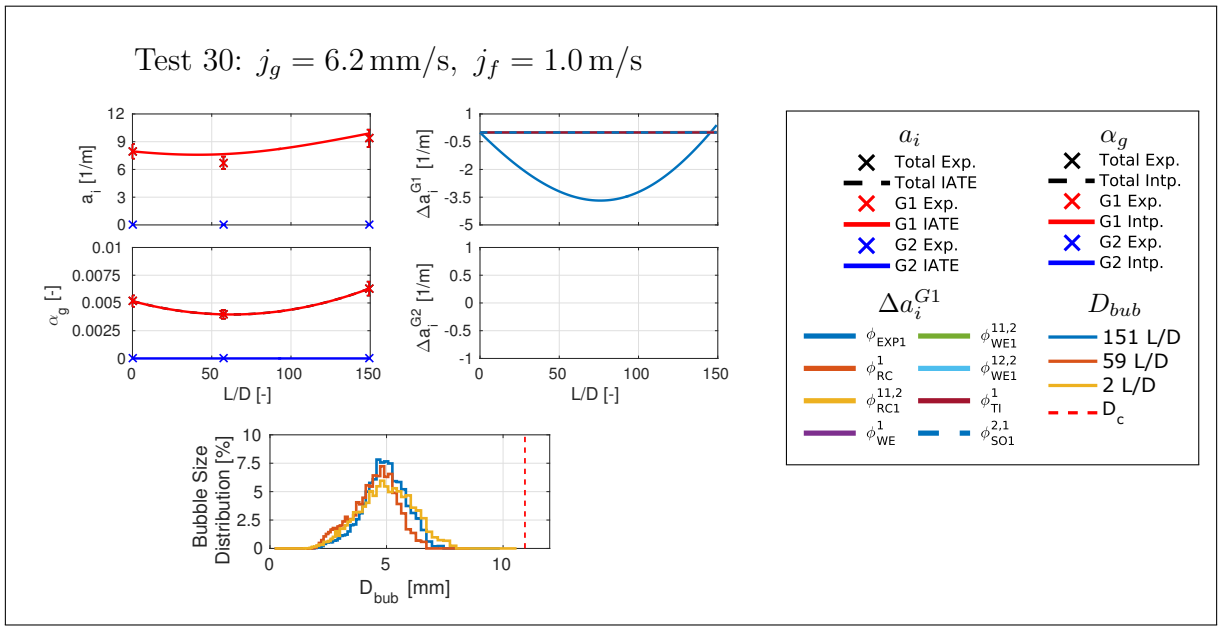

Figure 5: Results for Test 30 using the 2G IATE model.

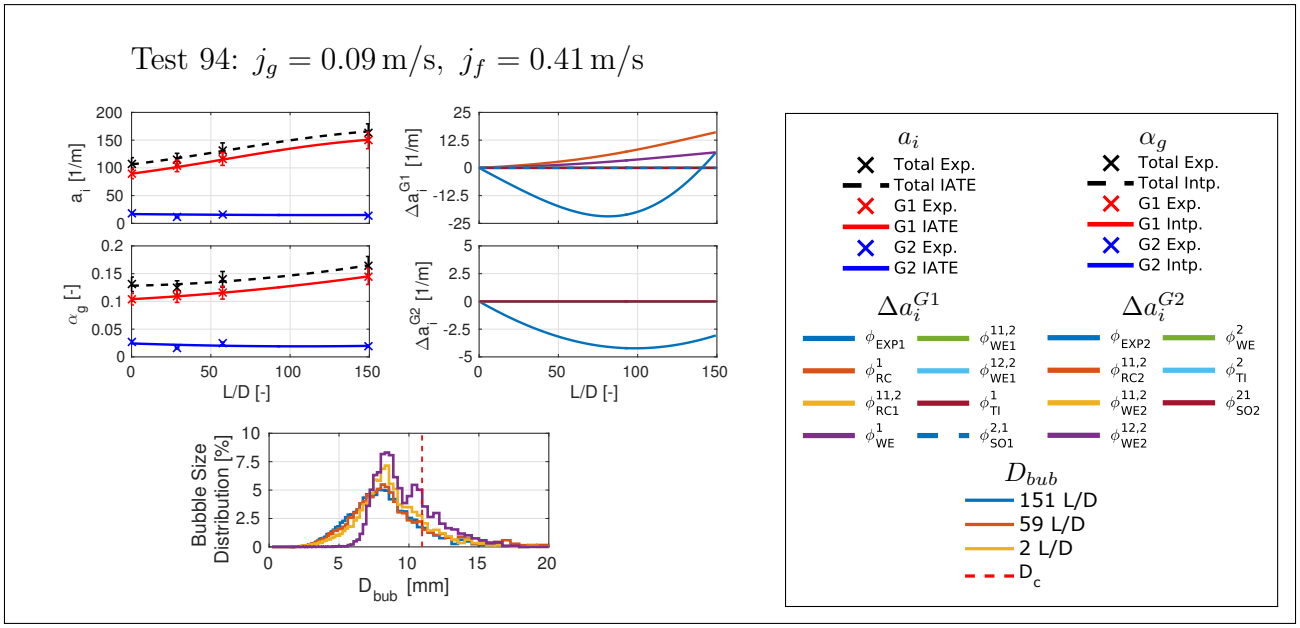

Figure 6: Results for Test 94 using the 2G IATE model. The critical diameter, D_c, indicated as the dashed red line, is the border between group-1 and group-2 bubbles.

Test 94, presented in Fig. 6, corresponds to moderate superficial gas and liquid velocities, and is close to the transition to slug flow regime. In this regime, both group-1 and group-2 bubbles are present in the flow and several bubble interaction mechanisms play a role in the propagation of the interfacial area concentration. The IATE model accurately predicts propagation of both group-1 and group-2 a_i values. The development of the bubble size distribution for group-1 tends to spread towards smaller bubble sizes and accounts for a majority of the entire bubble population. This indicates that break-up should be a dominating mechanism for group-1 bubbles and a

greater fraction of total a_i should be accounted for by smaller bubbles. For group-2, little change is noted in the shape of the bubble size distribution, indicating a relatively neutral a_i propagation. This is consistent with the evolution of a_i for group-2.

As discussed in Section 3.1, the IATE performance increasingly deteriorates when approaching the transition to slug flow regime. To gain more insight into the reasons for performance deterioration, Tests 115 to 119 corresponding to a constant $j_g = 0.22\,\mathrm{m/s}$ and varying superficial liquid velocities are presented in Fig. 7. These tests are specifically chosen as they capture the gradual transition from the bubbly flow regime to the slug flow regime (refer to Table 4). For $j_f = 1.6\,\mathrm{m/s}$, the group-wise a_i values are predicted well. As noted in previous successful tests, the bubble expansion is the major source/sink – further supported by the experimental bubble size development. At $j_f \leq 0.64\,\mathrm{m/s}$, there are several interaction mechanisms that are invoked for group-1 a_i transport. The summation of the interaction mechanisms $\phi^{2,1}_{SO1}$, ϕ^{1}_{RC}, ϕ^{1}_{WE}, $\phi^{12,2}_{WE1}$ together with bubble expansion results in a successful prediction of group-1 a_i both qualitatively and quantitatively. Meanwhile, the propagation of group-2 a_i is dominated by a single interaction mechanism, ϕ^{2}_{WE} – the wake entrainment of a group-2 bubble into another group-2 bubble. The ϕ^{2}_{WE} term causes a strong over-prediction of group-2 bubble coalescence and nullifies its a_i value. The experimental bubble size distribution of group-2 bubbles ($D_{bub} > D_c$) tends to smear and increase in mean value to higher diameters; this indicates that there may indeed be significant coalescence occurring among group-2 bubbles.

The $j_f = 1.0\,\mathrm{m/s}$ test has been neglected in the discussion above. The test has interesting implications as it only has bubble expansion as dominating a_i source/sink yet achieves poor quantitative prediction. This result is in contrast to the tests discussed thus far. This may be indicative of IATE failing to completely capture the transition from a j_g–j_f space that is purely pressure-head driven to regimes involving a combination of bubble expansion and bubble interaction mechanisms.

The wake entrainment of group-2 bubbles is expected to be a major coalescence mechanism in the Fu-Ishii model [8]. It is mechanistically modelled by simplifying the interaction to be one-dimensional (in the axial direction), which is a valid assumption for small-diameter pipes. Experimentally, a trailing bubble is observed to accelerate when it enters the wake formation of a leading bubble. Due to a lack of understanding of the complex fluid-dynamics in the wake region, no theoretical formulation for the rise velocity exists. In lieu, empirical correlations for the rise velocity of a Taylor bubble [30] and a critical entrainment distance (approximately $6D$ [3]) are used to estimate the average entrainment collision frequency. The total entrainment rate between group-2 bubbles, S^2_{WE} is proportional to the number density distribution, f_2, of group-2 bubbles. The number density distribution is estimated as a flat distribution which is proportional to α_2, therefore $S^2_{WE} \propto \alpha_2$. This relation is realized in the results; with decreasing j_f, the void fraction of group-2 increases, accompanied by an increase in the sink term due to wake entrainment, ϕ^2_{WE}. Since this paper's implementation of the IATE model (see Section 1.3) utilizes experimental data for void fraction, the impact of wake entrainment (or any other mechanisms) has no effect on void fraction propagation. Due to the decoupling of a_i and α_g, a strong insertion of wake entrainment sink for group-2 is still noted after group-2 a_i nullifies.

Analyzing the results obtained for a fixed liquid superficial velocity and different gas superficial velocities, it is evident that problems arising from wake entrainment of group-2 are not isolated to a single region in the j_g–j_f space. In Fig. 8, results are shown for a series of tests characterized by constant $j_f = 1.0\,\mathrm{m/s}$ and increasing j_g. The prediction of a_i is good both qualitatively and quantitatively for $j_g \leq 0.14\,\mathrm{m/s}$. Similar to the discussion above, at high superficial gas to liquid velocity ratios ($j_g \geq 0.34\,\mathrm{m/s}$) there is poor prediction of group-2 a_i caused by an over-prediction of the sink term ϕ^2_{WE}. Furthermore, a similar transitional region is noted for $j_g = 0.22\,\mathrm{m/s}$ where an expansion dominating sink/source is insufficient in quantitatively predicting a_i propagation.

The prediction of group-1 interfacial area concentration is overall in good agreement with the experimental data, both quantitatively and qualitatively. Aside from the bubble expansion term, the dominating group-1 interaction mechanism (for both Figs. 7 and 8) is the shearing-off mechanism. This mechanism is expected to be a major a_i

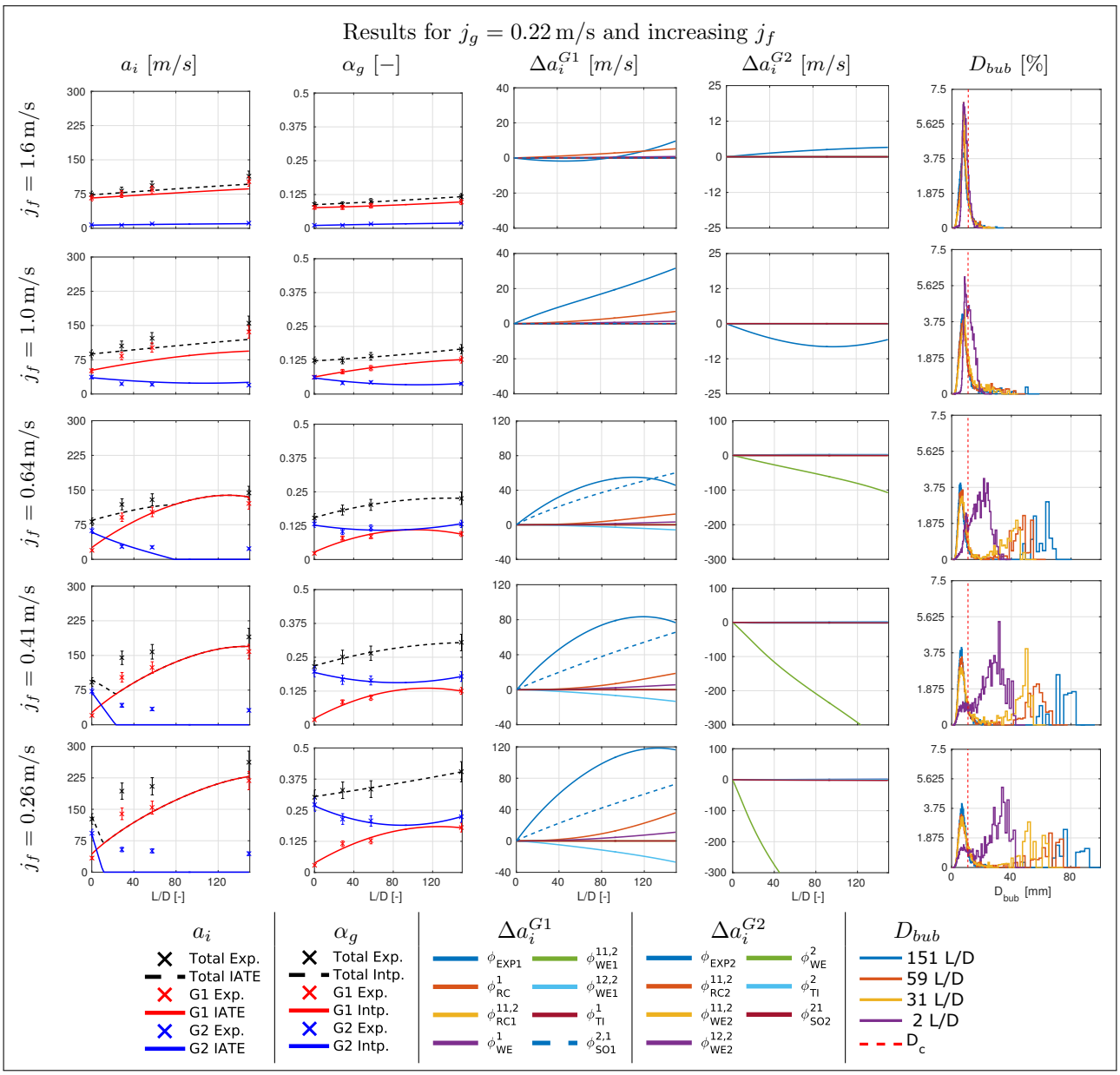

Figure 7: Results for Tests 115 to 119 using the 2G IATE model.

source for group-1 bubbles, if there exists large group-2 bubbles in the flow. Therefore the term $\phi_{SO1}^{2,1}$ is proportional to the group-2 void fraction, α_g^{G2}. The usage of experimental void fraction values allows access to accurate group-2 void fraction values and therefore the magnitude of shearing-off. Under the assumption that the magnitude of other minor group-1 interaction mechanisms are predicted well, the mechanistic and empirical modelling of shearing-off is successful.

A brief discussion of total a_i prediction is also warranted. As noted in Fig. 4, the total a_i performance is a blend of group-wise a_i performance. Through observations of tests in Figs. 7 and 8 this occurs due to two reasons. In tests where group-1 a_i is dominating the total a_i, there tend to be few active interaction mechanisms and the propagation of a_i is expansion driven. Tests in which there is a high initial group-2 a_i, the group-2 contribution tends to decrease and reach an equilibrium fast, whereas the group-1 a_i sees an exponential increase. As discussed previously, since there is a good prediction of group-1 a_i, this leads to a relatively good prediction of total a_i. This distinction in group-wise and total performance is important as typical best-estimate thermal-hydraulic system

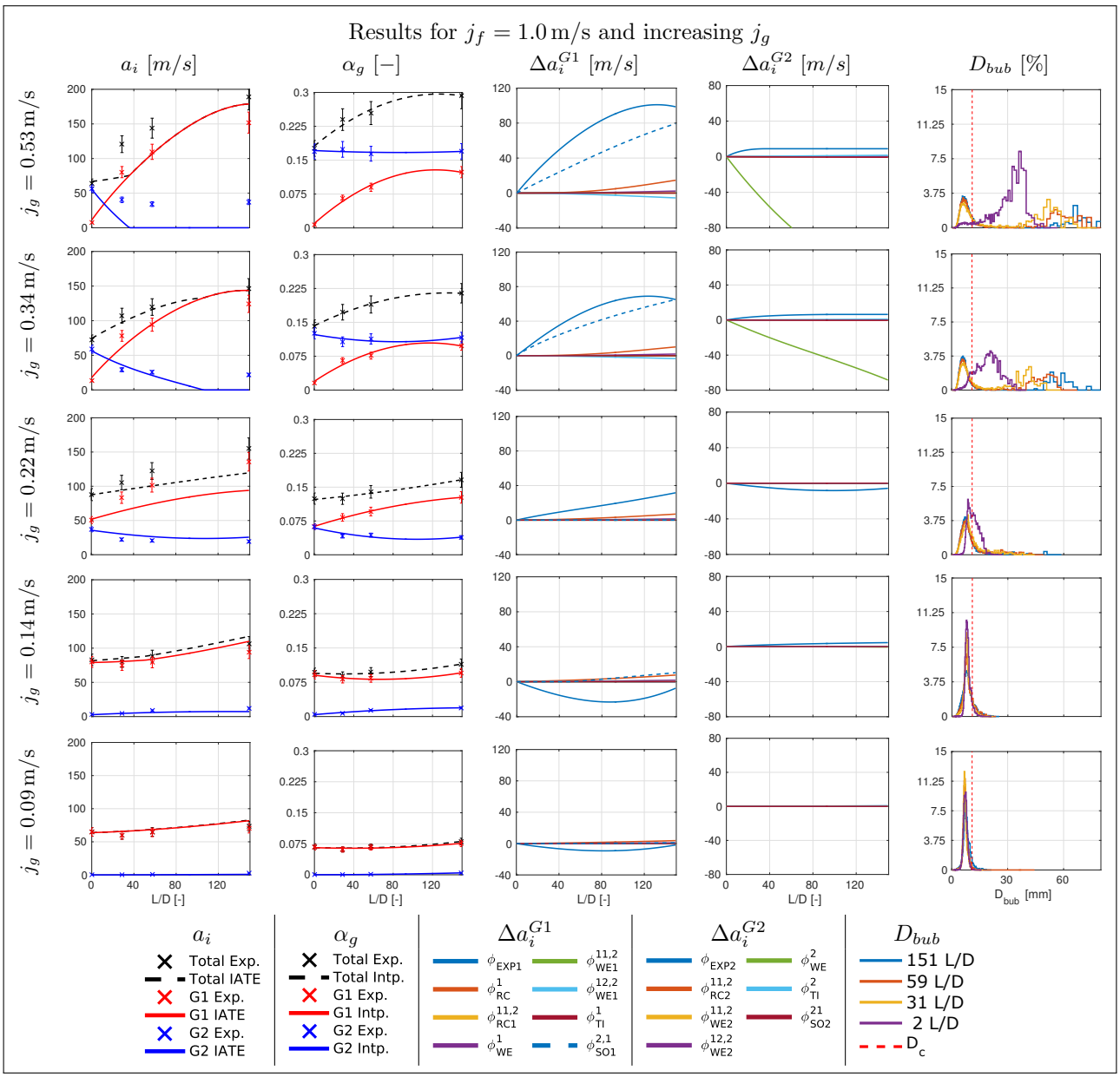

Figure 8: Results for Tests 96, 107, 118, 129, and 140 using the 2G IATE model.

codes only require total a_i, while newly proposed formulations of the two-fluid models [45] require group-wise a_i values.

3.3. Sensitivity analysis of IATE model coefficients

The performance of the Fu-Ishii 2G IATE model varies with respect to the multiphase flow regime. In the bubbly flow regime there is excellent performance, owed to the domination of group-1 bubbles and their propagation solely due to pressure drop expansion. As detailed in Section 3.2, at the onset of slug flow regime and onward, large group-2 bubbles play an increasingly dominating role in the contribution towards total interfacial area. Several postulated interaction mechanisms aim to predict the increase/decrease in the group-2 bubble population. The wake entrainment of group-2 bubbles (i.e. the coalescence of a trailing group-2 bubble into a leading group-2 bubble) was a detrimental mechanism. The strong sink insertion from ϕ^2_{WE} leads to a significant deterioration of the group-2 a_i prediction in high void fraction flow regimes.

In order to quantitatively isolate sources of poor performance, a sensitivity analysis of the Fu-Ishii model coefficients (refer to Table 2) was conducted. The sensitivity analysis considers the average error, Eq. (7), in prediction of interfacial area for all TOPFLOW DN50 tests. Each coefficient in the model is perturbed incrementally and then entire experimental test matrix (refer to Table 4) is evaluated with the modified coefficient. The evaluation process is repeated for a total of 10,000 uniform log-normally distributed perturbations, for each coefficient. The range of perturbation spans 4 orders of magnitude about the default coefficient value.

A principal component analysis (PCA) [18] allows quantitative evaluation of the IATE performance sensitivity with respect to coefficient perturbations. The PCA algorithm assesses the observation matrix generated for sensitivity analysis (i.e. a matrix with 60,000 sets of all perturbed coefficients). In this work, each observation is weighted by the inverse of the average error (in prediction of interfacial area for all TOPFLOW DN50 tests). For example, a coefficient set that performs well (and therefore has a low error) will have a greater weight. The output of the PCA is a new orthogonal set of principal axes that account for the greatest *improvement* in error. The principal axes of the IATE model is presented in Table 5. The cumulative variance for $\vec{PC}_1$ is 0.999, indicating that 99.9% of variance in the observations can be projected onto the first principal axes. The main component of $\vec{PC}_1$ is the coefficient of wake entrainment for group-2 bubbles, C^2_{WE}. Therefore, the output of PCA indicates that the improvement in performance of the Fu-Ishii model for TOPFLOW DN50 conditions is *highly sensitive* to the value of C^2_{WE}.

Table 5: First three principal components of Fu-Ishii 2G IATE coefficients for the prediction of TOPFLOW DN50 interfacial area propoagation.

	$\vec{PC}_1$	$\vec{PC}_2$	$\vec{PC}_3$	...
C_{RC}	0.000	0.002	0.048	...
C_{TI}	0.004	1.000	0.002	...
C_{WE}	0.000	0.001	-0.019	...
$C^{12,2}_{WE}$	0.001	0.002	0.999	...
C^2_{WE}	1.000	0.004	0.001	...
C_{SO}	0.000	0.000	0.001	...
$\sum \sigma^2$	0.999	1.000	1.000	...

The assertion that C^2_{WE} plays an important role in the improvement of the Fu-Ishii model is supported by discussion of individual tests in Section 3.2. In the individual tests, it was noted that poor performance of group-2 bubbles was dominated by the wake entrainment of large group-2 bubbles. Physically, it is expected [8] that wake entrainment of larger bubbles would be a dominating mechanism in small diameter pipes. In small pipes, increasingly large bubbles are quickly constrained by the cross-sectional area and participate in few interaction mechanisms. Thus, the wake entrainment of large bubbles is the dominating coalescence mechanism. The sensitivity analysis indicates that varying the magnitude of C^2_{WE} has the largest impact on the performance of the Fu-Ishii model. The coefficient C^2_{WE} only directly impacts the coalescence of large group-2 bubbles. As we expect this mechanism to dominate physically, it can be inferred that a revaluation of C^2_{WE} would be important in extending the range of the Fu-Ishii model for small diameter pipes.

The PCA output also indicates that coefficients other than C^2_{WE} have an almost negligible sensitivity on the improvement of the IATE model. This could indicate two different circumstances. One is that the established magnitude of the coefficients (refer to Table 2) accurately predict bubble interaction mechanisms and that altering their value would deter performance. An example of such a coefficient would be C_{SO}, the coefficient for the shearing-off mechanism. In Figs. 7 and 8, the prediction of group-1 a_i is good and the leading source is $\phi^{2,1}_{SO}$, representing the shearing-off mechanism. The PCA suggests, quantitatively, that any modification of C_{SO} would cause a deterioration in performance. Thus, any increase or decrease of C_{SO} would respectively lead to over-prediction or under-prediction

of group-1 a_i, *on average*. As observations are weighted by the inverse of the average error, it is understandable that the PCA indicates low sensitivity to changes in magnitude of C_{SO}. A similar argument can be made for the coefficient of random collision, C_{RC}, which has a lesser impact on group-1 and group-2 a_i propagation. The other circumstance is that any change in coefficient value has no impact on performance because the driving rate of coalescence/break-up is zero. Coefficients that would fall into this category include: the coefficient for turbulent impact C_{TI}, the coefficient for wake-entrainment of group-1 bubbles C_{WE}, and the coefficient for wake-entrainment of group-1 and group-2 into group-2 bubbles, $C_{WE}^{12,2}$. The negligible impact of these mechanisms on the successful prediction of a_i, is expected [8]. For small diameter pipes, the turbulent impact mechanism is expected to play a negligible role. Furthermore, out of all the possible wake entrainment interactions, only the group-2 mechanism (ϕ_{WE}^2) is expected to have a dominating impact in smaller pipes.

4. Optimization Study

The evaluation of the WMS database indicated performance in the high void fraction regime was poor. The sensitivity analyses indicated that wake entrainment of large bubbles is the major culprit. In this section, an optimization algorithm is utilized to seek an improvement. The WMS data will be the basis for the optimization process. Afterwards, the optimized model will be evaluated against all other databases available in the literature. First, the evaluation of the unmodified Fu-Ishii model against all databases is summarized in Section 4.1. The optimization methodology is noted in Section 4.2. The results from the optimization are presented in Section 4.3.

4.1. Evaluation of all databases

The proceeding figures and tables will concurrently present evaluations of TOPFLOW DN50 data, and Purdue University data. In Table 3, the TOPFLOW DN50 wire-mesh sensor data is noted as Prasser [38] (52.3 mm). The Purdue University needle probe data is noted as Ishii [17] (12.7 mm), Fu [7] (48.3 mm), and Ishii [17] (102 mm). All discussions will mention performance, of which the figure of merit is the error, defined by Eq. (7).

A compilation of the default performance of the Fu-Ishii model is presented in Fig. 9. For the TOPFLOW DN50 tests, it was found that the IATE model performs well for group-1 bubbles, but that the performance deteriorates as the flow conditions move toward the slug flow regime. The prediction of group-2 a_i is generally poor. The wake entrainment mechanism for group-2 bubbles is the major contributor towards over-prediction of interfacial area sink. The Purdue University experiments have similar performance in the $j_g - j_f$ space, and thus flow regimes. There is generally good performance for group-1 a_i prediction. The group-2 a_i propagation is poorly predicted, with error generally above 40%. The average error, binned by superficial velocities, is tabulated in Table 6. For TOPFLOW data, the error remains below 20% for $j_g < 2 \cdot 10^{-1}$ m/s; it is substantially higher at high j_g. Similar errors are noted for Purdue 48.3 mm data. For 12.7 mm and 102 mm data, it is interesting to note that while the group-1 and total interfacial area is predicted well, the group-2 interfacial area is still predicted poorly.

In summary, the Fu-Ishii two-group IATE model generally performs well for prediction of group-wise and total interfacial area at low superficial gas velocities. For flow conditions with $j_g \geq 2 \cdot 10^{-1}$ m/s, larger group-2 bubbles appear in the flow. In general, the contribution of these larger bubbles to the overall interfacial area concentration is not adequately predicted. In particular, a significant disagreement with group-2 bubbles experimental data is found for both TOPFLOW DN50 (52.3 mm) and Purdue 48.3 mm database – suggesting some dependence of the IATE performance on the hydraulic diameter.

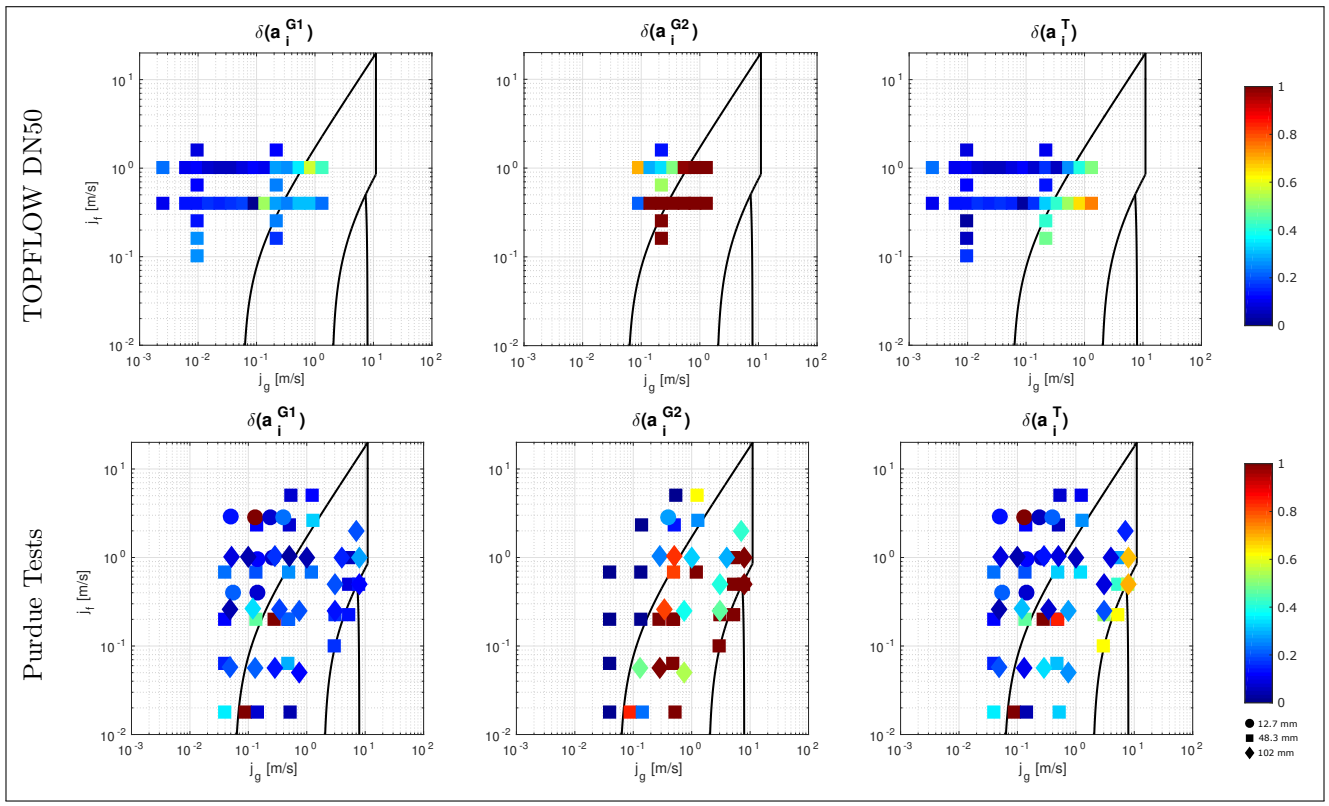

Figure 9: Error in prediction of interfacial area for the default Fu-Ishii model.

Table 6: A comparison of average error calculated by Eq. (7) for the default Fu-Ishii model.

			$j_g \leq 10^{-2}$ m/s	10^{-2} m/s $< j_g < 2 \cdot 10^{-1}$ m/s	$j_g \geq 2 \cdot 10^{-1}$ m/s
TOPFLOW 52.3 mm	$j_f \geq 5 \cdot 10^{-1}$ m/s	G1	13.2	7.92	31.8
		G2	0.00	16.6	63.9
		T	13.2	7.34	23.4
	$j_f < 5 \cdot 10^{-1}$ m/s	G1	17.1	20.0	25.0
		G2	0.00	20.2	100
		T	10.4	13.4	50.6
Purdue 48.3 mm	$j_f \geq 5 \cdot 10^{-1}$ m/s	G1		17.7	14.6
		G2	N/A	0.0	64.7
		T		17.7	26.6
	$j_f < 5 \cdot 10^{-1}$ m/s	G1		36.0	26.9
		G2	N/A	17.6	99.3
		T		35.4	54.8
Purdue 12.7, 102 mm	$j_f \geq 5 \cdot 10^{-1}$ m/s	G1		19.6	12.7
		G2	N/A	15.0	40.6
		T		19.7	13.8
	$j_f < 5 \cdot 10^{-1}$ m/s	G1		21.8	12.5
		G2	N/A	21.7	37.9
		T		17.8	12.6

4.2. Optimization Methodology

Various optimization algorithms are described in the open literature [4, 33]. The choice of optimization algorithm depends on the particular problem. The TOPFLOW DN50 experimental data are used as basis for the optimization. The following problem is posed:

$$\begin{aligned} \text{Minimize:} \quad & f(\vec{x}) \\ & \vec{x} \in \Re^n \\ \text{Given:} \quad & \vec{x}_{\min} \leq \vec{x} \leq \vec{x}_{\max} \end{aligned}$$

The objective function, $f(\vec{x})$, to be used in the optimization algorithm is the relative error between IATE model predictions of interfacial area concentration and the corresponding experimental data. The objective function is defined by

$$f(\vec{x}) \equiv \frac{1}{Z-1} \sum_{\zeta=2}^{Z} \left[\omega_{1,\zeta} \left| \frac{a_{1,\zeta,\text{calc}} - a_{1,\zeta,\text{meas}}}{a_{1,\zeta,\text{meas}}} \right| + \omega_{2,\zeta} \left| \frac{a_{2,\zeta,\text{calc}} - a_{2,\zeta,\text{meas}}}{a_{2,\zeta,\text{meas}}} \right| \right] , \tag{9}$$

where Z represents the total number of measured axial locations, and the subscripts indicate calculated (calc) or experimentally obtained (meas) values of the group-wise interfacial area concentration at location ζ. The group weighting factor,

$$\omega_{g,\zeta} \equiv \frac{a_{g,\zeta}}{a_{1,\zeta} + a_{2,\zeta}} \text{ where } g = (1,2) , \tag{10}$$

allows consideration of the importance of the group-wise interfacial area contribution towards the objective function. The input, $\vec{x}$ replaces default coefficients ($\vec{C}$) of the Fu-Ishii IATE model (the default coefficients of Fu-Ishii's model are presented in Table 2). The inputs are real and part of an n-dimensional domain, where n is the number of coefficients being modified, subject to varying boundaries. The lower boundary is currently set as 0 ($\vec{x}_{\min} = \vec{0}$). The upper boundary is set as two order of magnitudes larger than default values ($\vec{x}_{\max} = 10^2 \vec{C}$).

There are several requirements to solve the problem. The optimization algorithm should address a non-linear objective function. Furthermore, the optimization should be global in order to consider the entire input domain. The genetic algorithm [9] is a heuristic search algorithm that mimics the process of natural selection – it is part of a larger class known as evolutionary algorithms. The algorithm attempts to solve optimization problems with techniques inspired from the field of biology such as inheritance, mutation, migration and selection. Due to the solution methodology, the genetic algorithm meets the requirements necessary to solve a non-linear and global problem. It should be noted that although the genetic algorithm attempts to arrive at a global minimum, it does not guarantee such an outcome. Increasing the number of minimum generations can ameliorate this issue (the default minimum generations is quadrupled from 20 per n to 80 in this study).

Two operators are defined to assess the optimization process: the change in objective function between two sets of coefficients $\vec{C}_{\text{default}}$ and $\vec{C}_{\min}$,

$$\Delta \left(f(\vec{x}) \right) \equiv f(\vec{C}_{\text{default}}) - f(\vec{C}_{\min}) . \tag{11}$$

and the relative change for a particular coefficient,

$$\delta(C) \equiv \frac{C_{\min} - C_{\text{default}}}{C_{\text{default}}} . \tag{12}$$

The subscript default refers to the currently published values of the Fu-Ishii model coefficients (refer to Table 2). The subscript min refers to a coefficient set that is generated by the genetic algorithm as having globally minimal error.

The results from using the genetic algorithm is presented next. In Section 3.3, it was found that a single interaction mechanism is responsible for the poor performance of the default IATE model in the high void fraction regime, namely the wake entrainment of large group-2 bubbles. Therefore, the objective function considers a small subset of all TOPFLOW DN50 tests that exhibit strong deterioration due to this mechanism.

4.3. Optimization Results

It has been determined that the largest improvement of the Fu-Ishii two-group IATE model is obtained by modifying the group-2 wake entrainment coefficient, C_{WE}^2 (referring to Section 3.3). Thus, a local subset of tests

among the TOPFLOW data are selected that exhibit a strong group-2 wake entrainment. In particular, tests 105, 114, 115, 116, 117, and 127 are considered by the objective function (refer to Table 4). These tests have experimental conditions that are alike, in terms of superficial velocities. Therefore, it is expected that optimizing the group-2 wake entrainment coefficient on these tests should improve performance in other tests at high void fractions.

The results from the optimization are presented in Table 7. The value of the objective function, Eq. (9), is improved by over 40%, and the value of the group-2 wake entrainment coefficient is decreased by 95%. The results of using the optimized C^2_{WE} coefficients are presented in Fig. 10 for all tests. The TOPFLOW tests will be discussed first. A majority of the improvement in performance occurs in the high void fraction region for group-2 bubbles. This manifests in a significant improvement in the total interfacial area prediction. The group-1 performance is not expected to change drastically. Changes in average error is tabulated in Table 8. Quantitatively, negligible changes in performance are noted for $j_g < 2 \cdot 10^{-1}$ m/s. For $j_g \geq 2 \cdot 10^{-1}$ m/s $\cap$ $j_f < 5 \cdot 10^{-1}$ m/s, significant improvement is noted resulting in about 33% improvement in total a_i prediction.

Table 7: Results for localized optimization of group-2 wake entrainment.

	C^2_{WE}	$f(\vec{x})$
Default	10.0	1.31
Optimized	0.515	0.875
δC	-0.95	$\Delta(f(\vec{x})) = 0.435$

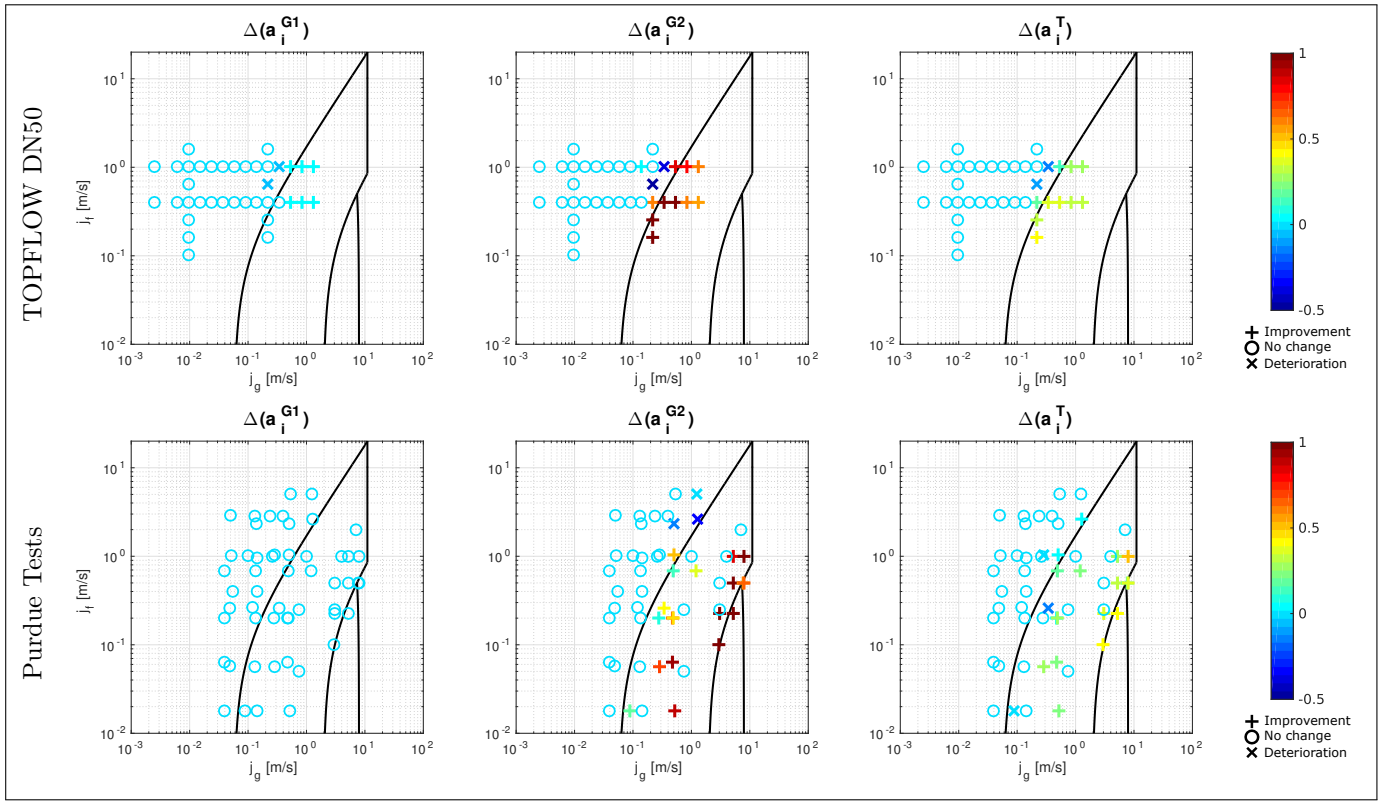

Figure 10: Improvement in Fu-Ishii model performance when using optimized C^2_{WE}.

When the optimized C^2_{WE} coefficient is applied to Purdue tests the outcome is positive. Fig. 10 also presents the individual change in performance for all Purdue tests. Similar to TOPFLOW, the prediction of group-1 interfacial area concentration sees no degradation/improvement, and the prediction of group-2 a_i improves mostly in the higher void fraction region. Table 8 also tabulates the change in average error for Purdue University tests. For the 48.3 mm

tests, a significant margin of 24% improvement for the total a_i is observed for high superficial gas to velocity ratio region, while no degradation in performance is noted on average. For the 12.7 mm and 102 mm tests, there are small increases in performance.

Table 8: Average error gain/loss calculated by Eq. (7) for all tests using optimized C^2_{WE}. The color reflects a nominal decrease or increase in relation to error values presented in Table 6.

			$j_g \leq 10^{-2}$ m/s	10^{-2} m/s $< j_g < 2 \cdot 10^{-1}$ m/s	$j_g \geq 2 \cdot 10^{-1}$ m/s
TOPFLOW 52.3 mm	$j_f \geq 5 \cdot 10^{-1}$ m/s	G1	0.0	0.0	0.1
		G2	0.0	0.3	16.1
		T	0.0	0.0	6.3
	$j_f < 5 \cdot 10^{-1}$ m/s	G1	0.0	0.0	1.2
		G2	0.0	0.0	60.4
		T	0.0	0.1	32.7
Purdue 48.3 mm	$j_f \geq 5 \cdot 10^{-1}$ m/s	G1	N/A	0.0	0.0
		G2		0.0	19.0
		T		0.0	13.3
	$j_f < 5 \cdot 10^{-1}$ m/s	G1		0.0	0.1
		G2		3.0	59.0
		T		0.0	24.0
Purdue 12.7, 102 mm	$j_f \geq 5 \cdot 10^{-1}$ m/s	G1	N/A	0.0	0.0
		G2		0.0	7.9
		T		0.0	3.8
	$j_f < 5 \cdot 10^{-1}$ m/s	G1	N/A	0.0	4.8
		G2		0.0	7.4
		T		0.1	1.1

The application of optimized C^2_{WE} to several TOPFLOW tests is shown in Fig. 11. As described in the previous section, tests 115 to 118 suffer from an increasing over-prediction of group-2 wake entrainment as the gas superficial velocity increases. On the right hand side of the figure, the corresponding results with the optimized C^2_{WE} are presented. For the cumulative group-2 source contribution ($\Sigma\phi_{j2}$), there is a significant reduction in the contribution from ϕ^2_{WE}, as expected. The optimization significantly improves the qualitative prediction of group-2 a_i. The total interfacial area is also propagated correctly within the experimental uncertainty bars at low L/D. The propagation of group-1 a_i is affected marginally. Group-1 a_i is most sensitive to changes in C^2_{WE} when the population of group-2 bubbles is significant and shearing-off occurs. An increased incidence of shearing-off, $\phi^{2,1}_{SO}$, increases the group-1 population, and thus its a_i.

The optimization of the C^2_{WE} coefficient based on a limited selection of tests (where the respective mechanism is prevalent) has a positive outcome on the entire $j_g - j_f$ space – irrespective of the experimental database. The reduction of C^2_{WE} from the default value of 10.0 to 0.515 results in only gains in performance for all databases. The studies have shown that while the magnitude of improvement in performance for alike hydraulic diameters is similar, a significantly lesser improvement is noted for smaller or larger diameters. Due to scaling effects, with respect to the hydraulic diameter, there is a limit to the universality of optimized coefficients that can be reasonably achieved.

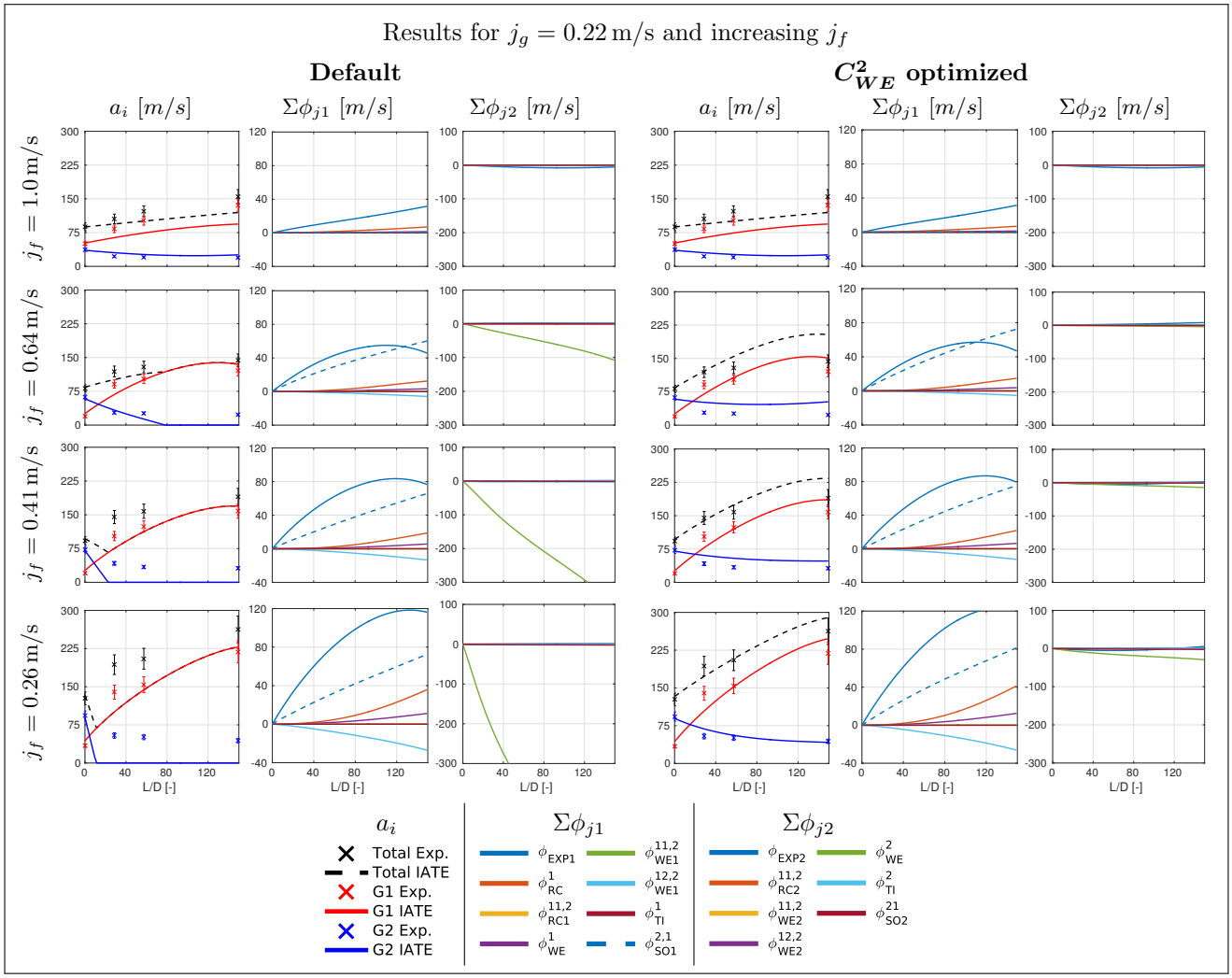

Figure 11: Results for Tests 115 to 118 using the 2G IATE model. The three left columns display results using default model coefficients. The three right columns display results using the optimized C^2_{WE} coefficient.

5. Conclusions

The interfacial area transport equation model (IATE) was developed in an attempt to address the drawbacks of the static regime flow maps, which is used widely for the two-fluid model closure. Initial experimental efforts and validation presented in the literature have focused on measurements in air-water experiments using conductivity probes. The present study is focused on the independent assessment of the two-group Fu-Ishii IATE performance for a small (52.3 mm) diameter pipe in various flow conditions, using a high-resolution and high-frequency wire-mesh sensor to experimentally characterize the liquid/gas interface.

The performance of the two-group IATE has been successful in low void fraction bubbly flows. In such flows, the bubble expansion term dominates the propagation of interfacial area. At high superficial velocities, where interaction mechanism source/sink terms are expected to contribute to interfacial area transport, the IATE performance deteriorates with increasing superficial gas to liquid velocity ratio. The sink for group-2 bubbles is over-predicted by the wake entrainment mechanism, leading to overall poor prediction of the total interfacial area concentration. A sensitivity analysis of the Fu-Ishii model coefficients indicates that a re-evaluation of the coefficient for group-2 wake entrainment, C^2_{WE}, would significantly improve performance. Group-1 interfacial area is predicted well in almost all tests. The shearing-off mechanism is a major source for group-1 a_i propagation if group-2 bubbles are present in the flow. Thus, the mechanistic modelling of the shearing-off mechanism has been successful.

In a study by Manera [28], it is noted that while the conductivity probe and wire-mesh sensor measurements are in good agreement for low void fractions, a significant discrepancy exists at high void fractions. The interfacial area concentration measured with conductivity probes is based on the measurement of the surface inclination with respect to the vertical axis. The measurement of such an angle is expected to deteriorate when the interface between phases is mostly parallel to the probes (such as in slug flows). In addition group-2 measurements might be affected by poor counting statistics. As the IATE model relies on empirically determined coefficients to close interaction mechanisms, the values require reassessment. The wire-mesh sensor has been benchmarked over a wide range of void fractions and is expected to retain accuracy in high void fraction flows. Therefore, the TOPFLOW data provides an avenue for addressing the shortcomings of the 2G IATE model.

The last portion of the paper implemented an optimization algorithm towards the reassessment of the group-2 wake entrainment. The optimization study focused on the modification of the group-2 wake entrainment coefficient (C^2_{WE}) on the basis of six neighboring TOPFLOW tests where an over-prediction of the incidence of group-2 wake entrainment mechanism was observed. The optimization resulted in a reduction of the default coefficient from 10.0 to 0.515. The modification of the group-2 wake entrainment coefficient resulted in a significant improvement in the prediction of the total a_i for TOPFLOW tests with $j_g \geq 2 \cdot 10^{-1}$ m/s, namely 6.3% for $j_f \geq 5 \cdot 10^{-1}$ m/s and 32.7% for $j_f < 5 \cdot 10^{-1}$ m/s. The application of the modified coefficient to Purdue 48.3 mm tests resulted in improvements of 13.3% and 24.0% for group-1 and group-2 a_i prediction, respectively. Application to other Purdue university tests (with smaller and larger diameters) indicated smaller improvement of 3.8% and 1.1% respectively, but negligible degradation in performance. While the optimization study has provided a path towards improvement, it has also indicated that the ceiling for improvement is dictated by the geometry of the experimental database used as a basis for the genetic algorithm and the lack of scalability of two-phase flow for larger or smaller pipe diameters.

Acknowledgements

The analyses presented in this work were sponsored by the United States Nuclear Regulatory Commission, grant No. NRC HQ 60 14 G 0008. The TOPFLOW experiments and the development of the original wire-mesh sensor software were carried out within the framework of research projects funded by the German Federal Ministry for Economic Affairs and Energy, project numbers: 150 1411 and 150 1329.

References

[1] M. Bernard, T. Worosz, S. Kim, C. Hoxie, and S. Bajorek. Comparison of results in the prediction of cap/slug flows between TRACE-T and TRACE V5.0 Patch 3. *The 15th International Topical Meeting on Nuclear Reactor Thermal Hydraulics*, 2013.

[2] AJ Dave, A Manera, M Beyer, D Lucas, and H-M Prasser. Uncertainty analysis of an interfacial area reconstruction algorithm and its application to two group interfacial area transport equation validation. *Nuclear Engineering and Design*, 2016.

[3] Abraham E Dukler, David Moalem Maron, and Neima Brauner. A physical model for predicting the minimum stable slug length. *Chemical Engineering Science*, 40(8):1379–1385, 1985.

[4] Emad Elbeltagi, Tarek Hegazy, and Donald Grierson. Comparison among five evolutionary-based optimization algorithms. *Advanced engineering informatics*, 19(1):43–53, 2005.

[5] DJ Euh, BJ Yun, CH Song, TS Kwon, MK Chung, and UC Lee. Development of the five-sensor conductivity probe method for the measurement of the interfacial area concentration. *Nuclear engineering and design*, 205 (1):35–51, 2001.

[6] Dongjin Euh, Basar Ozar, Takashi Hibiki, Mamoru Ishii, and Chul-Hwa Song. Characteristics of bubble departure frequency in a low-pressure subcooled boiling flow. *Journal of nuclear science and technology*, 47(7): 608–617, 2010.

[7] X. Y. Fu and M. Ishii. Two-group Interfacial Area Transport in Vertical Air–water Flow II. Model Evaluation. *Nuclear Engineering and Design*, 219(2):169–190, 2003.

[8] X. Y. Fu and M. Ishii. Two-group Interfacial Area Transport in Vertical Air–water Flow I. Mechanistic Model. *Nuclear Engineering and Design*, 219(2):143–168, 2003.

[9] David E. Goldberg. *Optimization & Machine Learning*. Addison-Wesley, 1989.

[10] G. F. Hewitt and N. S. Hall-Taylor. Annular two-phase flow, 1970.

[11] T. Hibiki and M. Ishii. Two-group interfacial area transport equations at bubbly-to-slug flow transition. *Nuclear Engineering and Design*, 202:39–76, 2001.

[12] Takashi Hibiki and Mamoru Ishii. Active nucleation site density in boiling systems. *International Journal of Heat and Mass Transfer*, 46(14):2587–2601, 2003.

[13] M. Ishii and T. Hibiki. *Thermo-Fluid Dynamics of Two-Phase Flow*. SpringerLink: Bücher. Springer New York, 2010. ISBN 9781441979858.

[14] M. Ishii and S. Kim. Development of One-group and Two-group Interfacial Area Transport Equation. *Nuclear Science Engineering*, 146(3):257–273, 2003.

[15] M. Ishii and K. Mishima. Two-fluid model and hydrodynamic constitutive relations. *Nuclear Engineering and design*, 82(2):107–126, 1984.

[16] M. Ishii and N. Zuber. Drag coefficient and relative velocity in bubbly, droplet or particulate flows. *AIChE Journal*, 25(5):843–855, 1979.

[17] M. Ishii, S. Kim, X. Y. Fu, T. R. Smith, S. S. Paranjape, X. Sun, H. Goda, J. Uhle, and J. Kelly. Experimental investigation of the interfacial area transport in vertical two-phase flow. Purdue University, 2003.

[18] Ian Jolliffe. *Principal component analysis*. Wiley Online Library, 2002.

[19] J. E. Kelly and M. S. Kazimi. Interfacial Exchange Relations for Two-Fluid Vapor-Liquid Flow A Simplified Regime Map Approach. *MIT Energy Laboratory Electric Utility Program*, (MIT-EL-81-024), 1981.

[20] S. Kim. *Interfacial Area Transport Equation and Measurement of Local Interfacial Characteristics*. PhD thesis, Purdue University, 1999.

[21] S Kim, XY Fu, X Wang, and M Ishii. Development of the miniaturized four-sensor conductivity probe and the signal processing scheme. *International journal of heat and mass transfer*, 43(22):4101–4118, 2000.

[22] G Kocamustafaogullari and M Ishii. Interfacial area and nucleation site density in boiling systems. *International Journal of Heat and Mass Transfer*, 26(9):1377–1387, 1983.

[23] G. Kocamustafaogullari and M. Ishii. Foundation of the interfacial area transport equation and its closure relation. *Inernational Journal of Heat and Mass Transfer*, 38(481), 1995.

[24] Yixiang Liao and Dirk Lucas. A literature review of theoretical models for drop and bubble breakup in turbulent dispersions. *Chemical Engineering Science*, 64(15):3389–3406, 2009.

[25] Yixiang Liao and Dirk Lucas. A literature review on mechanisms and models for the coalescence process of fluid particles. *Chemical Engineering Science*, 65(10):2851–2864, 2010.

[26] A. Manera. *Experimental and analytical investigations on flashing-induced instabilities in natural circulation two-phase systems*. PhD thesis, Delft University of Technology, 2003.

[27] A Manera, HM Prasser, THJJ Van der Hagen, RF Mudde, and WJM de Kruijf. A comparison of void-fraction measurements during flashing-induced instabilities obtained with a wire-mesh sensor and a gamma-transmission set-up. *ICMF-2001, New Orleans, May*, 2001.

[28] A. Manera, B. Ozar, S. Paranjape, M. Ishii, and H.-M Prasser. Comparison between wire-mesh sensors and conductive needle-probes for measurements of two-phase flow parameters. *Nuclear Engineering and Design*, 239:1718–1724, 2008.

[29] K. Mishima and M. Ishii. Flow regime transition criteria for upward two-phase flow in vertical tubes. *International Journal of Heat and Mass Transfer*, 27(5):723–737, 1984.

[30] R Moissis and P Griffith. Entrance effects in a two-phase slug flow. *J. Heat Transfer*, 84(1):29–38, 1962.

[31] Gustavo Montoya, Dirk Lucas, Emilio Baglietto, and Yixiang Liao. A review on mechanisms and models for the churn-turbulent flow regime. *Chemical Engineering Science*, 141:86–103, 2016.

[32] LG Neal and SG Bankoff. A high resolution resistivity probe for determination of local void properties in gas-liquid flow. *AIChE Journal*, 9(4):490–494, 1963.

[33] Panos M Pardalos and J Ben Rosen. *Constrained global optimization: algorithms and applications*. Springer-Verlag New York, Inc., 1987.

[34] Hyun-Sik Park, Tae-Ho Lee, Takashi Hibiki, Won-Pil Baek, and Mamoru Ishii. Modeling of the condensation sink term in an interfacial area transport equation. *International Journal of Heat and Mass Transfer*, 50(25): 5041–5053, 2007.

[35] H.-M Prasser, A. Böttger, and J. Zschau. A new electrode-mesh tomograph for gas–liquid flows. *Flow Measurement and Instrumentation*, 9, 1998.

[36] H-M Prasser, D Scholz, and C Zippe. Bubble size measurement using wire-mesh sensors. *Flow measurement and Instrumentation*, 12(4):299–312, 2001.

[37] H.-M Prasser, M. Misawa, and I. Tseanu. Comparison between wire-mesh sensor and ultra-fast X-ray tomograph for an air-water flow in a vertical pipe. *Flow Measurement and Instrumentation*, 16, 2005.

[38] H.-M Prasser, D. Lucas, M. Beyer, C. Vallee, E. Krepper, T. Hohne, A. Manera, H. Carl, H. Pietruske, P. Schutz, A. Zaruba, S. Al Issa, J.-M Shi, and F.-P Weib. Construction and execution of experiments at the multi-purpose thermal hydraulic test facility TOPFLOW for generic investigations of two-phase flows and the development and validation of CFD codes. *Wissenschaftlich-Technische Berichte*, FZD-481, 2007.

[39] Horst-Michael Prasser. Wire-mesh sensors for two-phase flow investigations. *Institute of Safety Research*, 23, 1999.

[40] J. P. Schlegel and T. Hibiki. A correlation for interfacial area concentration in high void fraction flows in large diameter channels. *Chemical Engineering Science*, 131:172–186, 2015.

[41] J. P. Schlegel, T. Hibiki, and M. Ishii. Two-group modeling of interfacial area transport in large diameter channels. *Nuclear Engineering and Design*, 293:75–86, 2015.

[42] S Sharaf, M Da Silva, U Hampel, C Zippe, M Beyer, and B Azzopardi. Comparison between wire mesh sensor and gamma densitometry void measurements in two-phase flows. *Measurement Science and Technology*, 22 (10):104019, 2011.

[43] Rong Situ, Mamoru Ishii, Takashi Hibiki, JY Tu, Guan Heng Yeoh, and Michitsugu Mori. Bubble departure frequency in forced convective subcooled boiling flow. *International Journal of Heat and Mass Transfer*, 51 (25):6268–6282, 2008.

[44] T. R. Smith, J. P. Schlegel, T. Hibiki, and M. Ishii. Mechanistic modeling of interfacial area transport in large diameter pipes. *International Journal of Multiphase Flow*, 47:1–16, 2012.

[45] X. Sun, M. Ishii, and J. M. Kelly. Modified two-fluid model for the two-group interfacial area transport equation. *Annals of Nuclear Energy*, 30(16):1601–1622, 2003.

[46] Xiaodong Sun, Seungjin Kim, Mamoru Ishii, and Stephen G Beus. Modeling of bubble coalescence and disintegration in confined upward two-phase flow. *Nuclear Engineering and Design*, 230(1):3–26, 2004.

[47] J. Talley, S. Kim, J. Mahaffy, S. Bajorek, and K. Tien. Implementation and evaluation of one-group interfacial area transport equation in TRACE. *Nuclear Engineering and Design*, 241(3):865–873, 2011.

[48] Weerin Wangjiraniran, Yuichi Motegi, Steffen Richter, Hiroshige Kikura, Masanori Aritomi, and Kazuhiko Yamamoto. Intrusive effect of wire mesh tomography on gas-liquid flow measurement. *Journal of nuclear science and technology*, 40(11):932–940, 2003.

[49] T. S. Worosz. *Interfacial Area Transport Equation for Bubbly to Cap-bubbly Transition Flows*. PhD thesis, Pennsylvania State University, 2015.

[50] Q Wu and M Ishii. Sensitivity study on double-sensor conductivity probe for the measurement of interfacial area concentration in bubbly flow. *International Journal of Multiphase Flow*, 25(1):155–173, 1999.

[51] Q Wu, S Kim, M Ishii, and SG Beus. One-group interfacial area transport in vertical bubbly flow. *International Journal of Heat and Mass Transfer*, 41(8):1103–1112, 1998.

[52] Zhiqiang Zhang, Martina Bieberle, Frank Barthel, Lutz Szalinski, and Uwe Hampel. Investigation of upward cocurrent gas–liquid pipe flow using ultrafast x-ray tomography and wire-mesh sensor. *Flow Measurement and Instrumentation*, 32:111–118, 2013.